AD NUMBER

AD474147

NEW LIMITATION CHANGE

TO

Approved for public release, distribution unlimited

FROM

Distribution authorized to U.S. Gov't. agencies and their contractors; Administrative/Operational Use; 28 JUL 1965. Other requests shall be referred to US Army Electronics Command, Attn: AMSEL-KL-EM, Fort Monmoyth, NJ.

AUTHORITY

USAEC ltr, 17 Dec 1965

Report No. 7
Seventh Quarterly Report

Covering the Period
1 March 1965 to 31 May 1965

Investigation of MICROWAVE DIELECTRIC-RESONATOR FILTERS

Prepared for:
U. S. ARMY ELECTRONICS LABORATORIES
FORT MONMOUTH, NEW JERSEY

CONTRACT NO. DA-36-039-AMC-02267(E)
TASK NO. IP6 22001 A 057 02

By: S. B. Cohn and E. N. Torgow

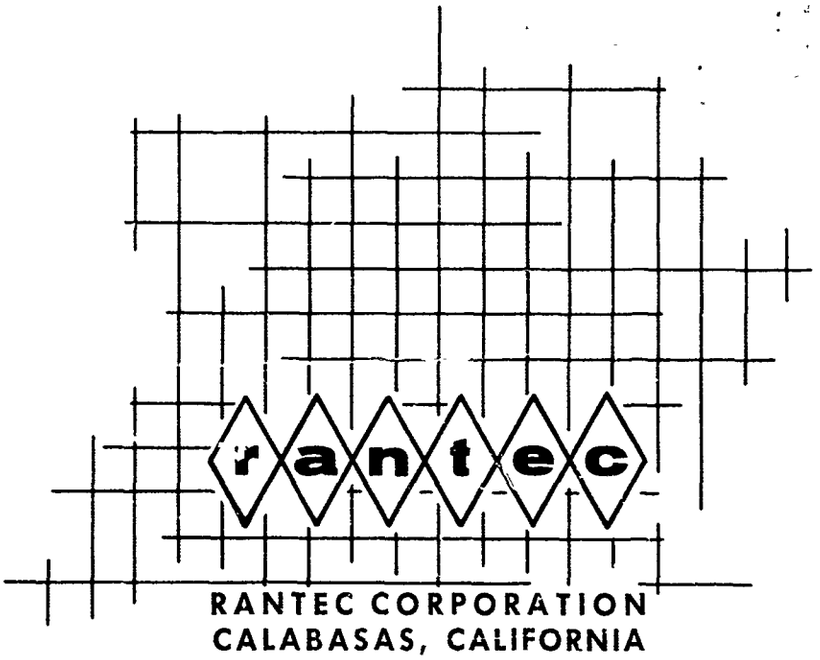

RANTEC CORPORATION
CALABASAS, CALIFORNIA

Report No. 7
Seventh Quarterly Report

Covering the Period
1 March 1965 to 31 May 1965

Investigation of MICROWAVE DIELECTRIC-RESONATOR FILTERS

Prepared for:
U. S. ARMY ELECTRONICS LABORATORIES
FORT MONMOUTH, NEW JERSEY

CONTRACT NO. DA-36-039-AMC-02267(E)
TASK NO. 1P6 22001 A 057 02

By: S. B. Cohn and E. N. Torgow

Rantec Project No. 31625

Approved:

Seymour B. Cohn

SEYMOUR B. COHN, Technical Director

TABLE OF CONTENTS

LIST OF ILLUSTRATIONS

LIST OF ILLUSTRATIONS (Cont'd)

SECTION I

PURPOSE

This program is intended to study the feasibility of high-dielectric-constant materials as resonators in microwave filters, and to obtain design information for such filters. Resonator materials shall be selected that have loss tangents capable of yielding unloaded Q values comparable to that of waveguide cavities. The materials shall have dielectric constants of at least 75 in order that substantial size reductions can be achieved compared to the dimensions of waveguide filters having the same electrical performance.

SECTION II

ABSTRACT

The subject of waveguide band-stop filters using dielectric resonators is considered in this report. Two basic orientations of a dielectric resonator in a TE_{10}-mode rectangular waveguide are analyzed. In one orientation, the equivalent magnetic-dipole moment of the dielectric resonator is transverse to the waveguide, and in the other it is axial. Formulas for external loaded Q are derived in both cases. Utilization of this Q_{ex} data in band-stop filter design is explained. An example is given of the design of a three-resonator band-stop filter, and the experimental response is shown to agree well with the anticipated performance.

Various configurations of dielectric resonators in waveguide that yield directional-filter performance are described in this report. In some of the cases, pairs of resonators operating in their fundamental mode are used. In other cases, a single resonator is used operating in its second mode of resonance. This mode in the case of a disk is a dual one, having two orthogonal resonant fields existing independently at the same frequency. When the disk is placed for proper directional-filter performance, the analysis shows the equivalent magnetic-dipole moment to be circularly polarized. Formulas are derived for several cases of particular interest. Methods of adding resonators to achieve multiple-resonator response are described.

Measured resonant-frequency curves are presented for the first three modes of a disk as a function of length-to-diameter ratio. Favorable regions of L/D yielding good mode separation are found in the cases of the first and second modes.

Data showing the effect of metal-wall proximity on unloaded Q and resonant frequency are presented for an axially oriented dielectric disk in square and circular cut-off tubes. Large disagreements with the previously derived approximate formulas are found, despite the fact that the analysis gave good results in the transverse case. An explanation for the failure of the theory is given, and it is shown how the accuracy of the analysis can be improved.

SECTION III

CONFERENCES AND PUBLICATIONS

On 5 May 1965, a paper on the subject of this study program was presented at the 1965 G-MTT Symposium, Clearwater, Florida, by Dr. S. B. Cohn. The title was "Microwave Filters Containing High-Q Dielectric Resonators."

A conference was held on 6 May 1965 at Clearwater, Florida. Those attending were Dr. S. B. Cohn and Mr. E. N. Torgow of Rantec Corporation and Messrs. J. Agrios and N. Lipetz of the U. S. Army Electronics Laboratories. Progress and future plans were reviewed.

SECTION IV

FACTUAL DATA

1. Introduction

Earlier work on this program has shown that a dielectric resonator placed in a propagating waveguide will produce a band-rejection response. A series of such resonators spaced at quarter or three-quarter wavelength intervals along the waveguide can be designed to yield a band-stop filter with a well-defined stop band and closely spaced well-matched upper and lower pass bands. Although it would have the same length as a conventional waveguide band-stop filter using side-coupled cavities, this dielectric resonator filter is of interest because it is wholly contained within the waveguide cross section. Also, the internal parts can be easily inserted without modification of the waveguide. A suitable length of straight waveguide would usually be available in most practical waveguide assemblies. Design formulas are derived in this report for waveguide band-stop filters containing dielectric resonators in various orientations, and an experimental example is presented.

A filter type of considerable practical interest is the directional filter. Directional filters are four-port devices that can be used to separate or combine adjacent frequency channels. Although the same effect can be achieved with a three-port device, the fourth port makes the directional filter applicable to more complex requirements, and also permits all ports to be reflectionless at all frequencies. This non-reflection property is not possible in a three-port lossless, reciprocal device. A number of dielectric-resonator configurations in waveguide are described in this report that can yield directional-filter performance. Design formulas are derived for the cases that appear to be of most practical interest.

A dielectric object can support an infinite number of resonant modes. In filters, only the first few modes would normally be of interest. Higher modes would be too closely spaced in frequency to be ordinarily useful. The lowest-frequency mode is generally preferred in band-pass and band-stop filters, but the work on directional filters shows the second resonant mode in a dielectric disk also to be of value. Measured resonant-frequency curves for the first three modes in a disk are given in this report as a function of length-to-diameter ratio. For good mode separation, this data reveals a broad range of permissible L/D in the case of the first mode, but only a narrow range in the case of the second mode.

In the Third Quarterly Report[1], experimental data were given for the effect of metal-wall proximity on the unloaded Q and resonant frequency of a dielectric resonator in a square metal tube of varying cross section. The configuration considered was transverse; that is, the axis of the disk was perpendicular to the axis of the square tube. Approximate equations were derived for wall proximity effects in the Sixth Quarterly Report.[2] Good agreement with the previous data was obtained for both Q_u and f_o. During the past quarter, measurements were made in the case of axial orientation of a disk in both square and circular tubes. The formulas of the Sixth Quarterly Report prove not as successful with the axial orientation, as compared with the transverse orientation. The source of error in the analysis believed responsible for the disagreement is discussed, and it is shown that the error should be expected to be large in the axial case, but small in the transverse case. The discussion shows the analysis to be capable of being extended to improve its accuracy.

2. Waveguide Band-Stop Filters

A dielectric resonator coupled to the H_x or H_z magnetic-field component of a propagating TE_{10} mode in rectangular waveguide will

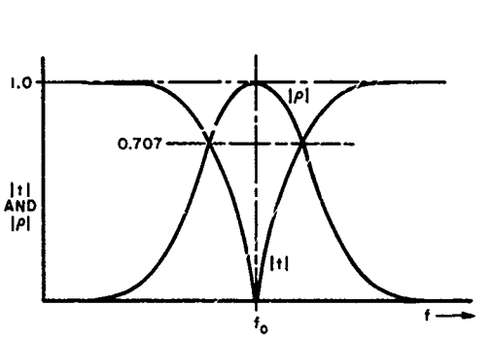

Figure 2-1. Transmission and Reflection Response of a Rejection Resonator

exhibit a band-stop response with essentially zero transmission coefficient and unity reflection coefficient at resonance. Typically the frequency response is as shown in Figure 2-1. This rejection effect in a propagating waveguide has been used earlier in the program as a convenient means of measuring the resonant frequency (f_o) and unloaded Q (Q_u) of dielectric samples.[3] Formulas will now be derived permitting the external loaded Q, Q_{ex}, to be computed as a function of the dimensions, dielectric constant, and resonant frequency of the dielectric object, the dimensions of the waveguide cross section, and the location and orientation of the dielectric object in the cross section.

When two or more resonators are used, spaced at odd-quarter-wave intervals along the waveguide, steeper and higher rejection can be achieved in the stop band and, at the same time, lower reflection in the pass band. In the Fifth Quarterly Report[4], the following design formula was given permitting the individual Q_{ex} values to be specified to achieve a desired bandwidth and response function. Although intended in the Fifth Quarterly Report for TEM-mode filters, the formula also applies to waveguide filters.

$$Q_{ex_i} = \frac{2}{\omega_1' w_1 g_i} \tag{2-1}$$

The notation is as shown in Figure 2-2. Q_{ex_i} is the Q factor of resonator number i placed by itself in a waveguide terminated by its characteristic impedance at both ends. The element values $g_i = g_1, g_2, \ldots, g_n$

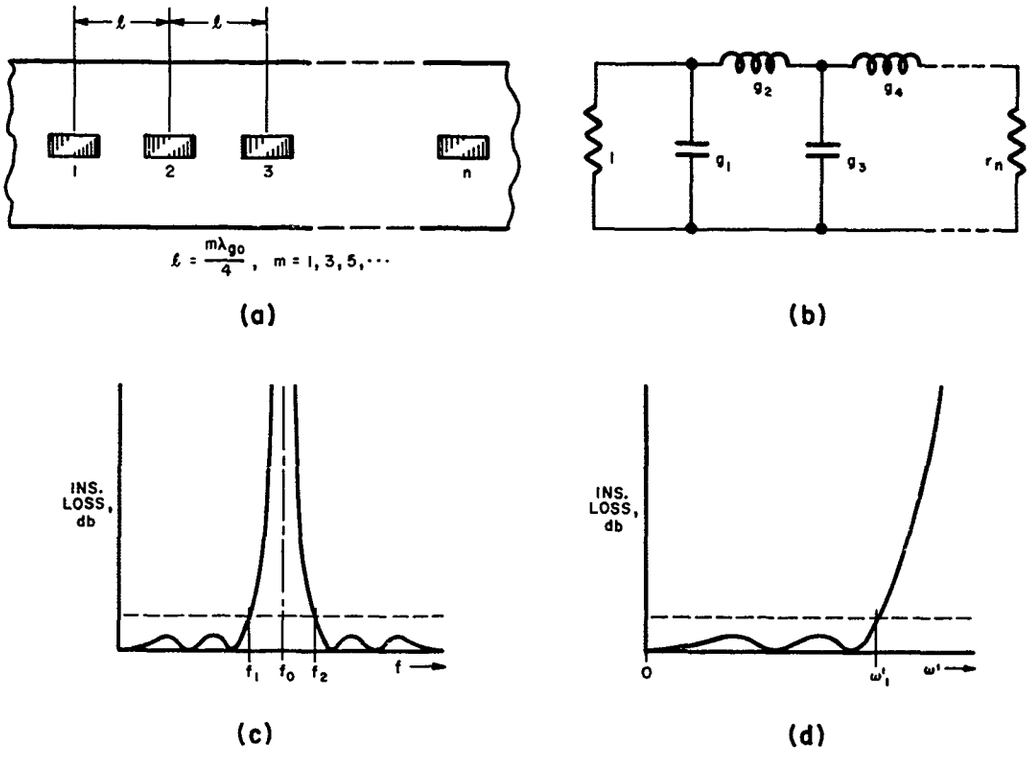

Figure 2-2. Waveguide Band-Stop Filter

apply to the prototype low-pass filter whose response function is to be simulated by the band-stop filter, $\omega' = 2\pi f'$ is the frequency function for the low-pass filter, and $w_1 = (f_2 - f_1)/f_o$ is the relative bandwidth of the band-stop filter. As shown in Figure 2-2, ω', w_1, f_1, and f_2 apply to corresponding response points of the low-pass and band-stop functions.

Formulas and tables of g_i for maximally flat and equal-ripple response functions have been published previously.[5,6] Note that the terminating-resistance value $r_n = 1$ shown in Figure 2-2 restricts the allowable equal-ripple cases to n = odd, only. To achieve an exact

equal-ripple response with n = even, either a transformer must be added to the band-stop filter at one end, or the characteristic impedance of the length of waveguide containing the resonators must be different from the terminating impedances.[6]

A formula yielding Q_{ex} of a single band-stop resonator will now be derived. As in previous analyses on this program, use will be made of the fact that the dielectric resonator appears at a distance to be a magnetic dipole of moment m proportional to the R-F H field at its center. For the rectangular-waveguide TE_{10} mode, there are two basic orientations of m to be considered: $m = m_x$ and $m = m_z$. The third possible orientation, $m = m_y$, produces no effect on the TE_{10} mode (since $H_y = 0$) and therefore is not of interest.

2.1 Case of $m = m_x$

An H-plane view of a dielectric resonator with m_x orientation in a rectangular waveguide is shown in Figure 2-3a. The TE_{10} wave components are shown in Figure 2-3b. The parameters in that figure are defined as follows: (1) the incident wave is E_{yi}; (2) the dipole moment induced by the incident wave is m_x; (3) the TE_{10} components excited by the dipole are E_y^- to the left and E_y^+ to the right; and (4) the total transmitted wave is E_{yt}. The phase reference in all cases is at the center of the dipole.

The transmission coefficient is

$$t = \frac{E_{yt}}{E_{yi}} = \frac{E_{yi} + E_y^+}{E_{yi}} \qquad (2\text{-}2)$$

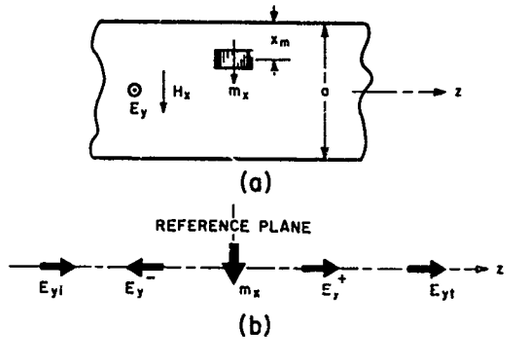

Figure 2-3. Case of Dielectric Resonator with $m = m_x$

and the reflection coefficient is

$$\rho = \frac{E_y^-}{E_{yi}} \tag{2-3}$$

At the resonant frequency, $t = 0$ and $|\rho| = 1$. Hence

$$E_y^+ = -E_{yi} \tag{2-4}$$

$$\left| E_y^- \right| = \left| E_{yi} \right| \tag{2-5}$$

The strength of the magnetic dipole, m_x, automatically adjusts itself to yield these results. The relationship between m_x and the waves E_y^+ and E_y^- may be obtained from an analysis in the Second Quarterly Report[7] that had been applied to a band-pass resonator in a nonpropagating waveguide. From that report, the wave components excited by m_x are

$$E_y^+ = a_{10} e_y e^{-j\beta z} \tag{2-6}$$

$$E_y^- = -a_{10} e_y e^{j\beta z} \tag{2-7}$$

$$H_x^+ = -\frac{\lambda}{\lambda_g \eta} E_y^+ \tag{2-8}$$

$$H_x^- = \frac{\lambda}{\lambda_g \eta} E_y^- \tag{2-9}$$

$$e_y = -\frac{\lambda_g \eta}{\lambda} h_x \tag{2-10}$$

$$h_x = \left(\frac{\lambda\beta}{ab\pi\eta}\right)^{1/2} \sin\frac{\pi x}{a} \tag{2-11}$$

$$a_{10} = -j\frac{\omega\mu_o m_x}{2}\left(\frac{\lambda\beta}{ab\pi\eta}\right)^{1/2} \sin\frac{\pi x_m}{a} \tag{2-12}$$

$$\eta = \sqrt{\frac{\mu}{\epsilon}} = 376.6 \quad \text{ohms} \tag{2-13}$$

$$\beta = \frac{2\pi}{\lambda_g} \tag{2-14}$$

$$k = \frac{2\pi}{\lambda} = \frac{\omega\mu}{\eta} \tag{2-15}$$

Hence, at $x = a/2$ and $z = 0$,

$$E_y^+ = -E_y^- = j\frac{k\eta m_x}{ab} \sin\frac{\pi x_m}{a} \tag{2-16}$$

$$H_x^+ = H_x^- = -j\frac{\beta m_x}{ab} \sin\frac{\pi x_m}{a} \tag{2-17}$$

The equivalent circuit of the resonant magnetic dipole in a propagating waveguide is shown in Figure 2-4. The definitions

$$V_g = 2E_{yi}b \tag{2-18}$$

$$Z_o = \frac{2\eta b\lambda_g}{a\lambda} \tag{2-19}$$

are arbitrary, but yield valid results since they are consistent on the following power basis:

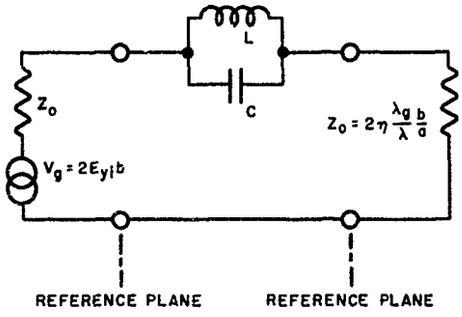

Figure 2-4. Equivalent Circuit for $m = m_x$

$$P_i = \frac{\int_0^b \int_0^a \left|E_{yi}\right|^2 \, dx \, dy}{2\eta} = \frac{(V_g/2)^2}{2Z_o} \tag{2-20}$$

where P_i is the power of the incident wave of amplitude E_{yi} or $V_g/2$.

In terms of the equivalent circuit, the Q of the resonant circuit loaded by both terminations is

$$Q_{ex} = \frac{\omega C}{\frac{1}{2} Y_o} = 2Z_o \omega C = \frac{4b\eta\lambda_g \omega C}{a\lambda} \tag{2-21}$$

At f_o, the voltage drop across the resonant circuit is equal to $V_g = 2E_{yi}b$. The energy stored in the resonant circuit is

$$W_m = W_e = \frac{1}{2} C \left|V_g\right|^2 = 2C \left|E_{yi}\right|^2 b^2 \tag{2-22}$$

which yields

$$C = \frac{W_m}{2\left|E_{yi}\right|^2 b^2} = \frac{W_m}{2\left|E_y^+\right|^2 b^2} \tag{2-23}$$

where Eq. 2-4, $E_y^+ = -E_{yi}$, was used. After combining Eqs. 2-16, 2-21, and 2-23, the following is obtained.

$$Q_{ex} = \frac{4b\eta\lambda_g\omega}{a\lambda} \cdot \frac{W_m}{2} \cdot \frac{a^2}{k^2\eta^2 m_x^2 \sin^2\left(\frac{\pi x_m}{a}\right)} \tag{2-24}$$

This may be rewritten with the aid of Eq. 2-15.

$$Q_{ex} = \left(\frac{2W_m}{\mu_o m_x^2}\right)\left(\frac{ab\lambda_g}{2\pi \sin^2\left(\frac{\pi x_m}{a}\right)}\right) \tag{2-25}$$

The first factor has occurred in several analyses in previous reports. Its reciprocal is designated by F, where

$$F = \frac{\mu_o m^2}{2W_m} \tag{2-26}$$

This parameter is a function of the shape, dimensions, and dielectric constant of the dielectric resonator itself. In the case of the fundamental resonance in a dielectric disk, F has been evaluated as follows:[7]

$$F = \frac{0.927\, D^4 L\epsilon_r}{\lambda_o^2} \; ; \; 0.25 \leq L/D \leq 0.7 \tag{2-27}$$

where D is diameter, L length, ϵ_r dielectric constant, and λ_o free-space resonant wavelength. Hence, the external Q of the x-oriented magnetic-dipole resonator is given by

$$Q_{ex} = \frac{ab\lambda_g}{2\pi F_x \sin^2\left(\frac{\pi x_m}{a}\right)} \tag{2-28}$$

The 3-db bandwidth of the single band-stop resonator is simply

$$w_{3db} = \frac{BW_{3db}}{f_o} = \frac{1}{Q_{ex}} \tag{2-29}$$

This may be confirmed through application of the equivalent circuit, Figure 2-4. The transmission coefficient is 0.707 (-3db) at the frequencies for which the reactance introduced by the L-C circuit is $X_{1,2} = \pm 2Z_o$. Therefore

$$B_{1,2} = \pm \frac{Y_o}{2} = \omega_{1,2}C - \frac{1}{\omega_{1,2}L} = \omega_{1,2}C\left(1 - \frac{f_o^2}{f_{1,2}^2}\right)$$

$$= \omega_{1,2}C \frac{\left(f_{1,2} + f_o\right)}{f_{1,2}} \cdot \frac{\left(f_{1,2} - f_o\right)}{f_{1,2}}$$

$$\approx \pm\omega_o C \cdot \left|\frac{f_2 - f_1}{f_o}\right| = \pm\omega_o C w_{3db} \tag{2-30}$$

and by Eq. 2-21,

$$w_{3db} \approx \frac{Y_o}{2\omega_o C} = \frac{1}{Q_{ex}} \tag{2-31}$$

2.2 Case of $m = m_z$

The m_z orientation in a rectangular waveguide is shown in Figure 2-5a. Equations 2-2 through 2-5 apply to this case as well

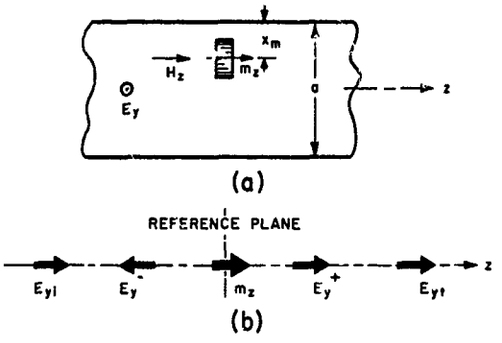

Figure 2-5. Case of Dielectric Resonator with $m = m_z$

as to the m_x case. However, with reference to the analyses in the Second and Fourth Quarterly Reports,[7,8] Eqs. 2-6 through 2-17 become

$$E_y^+ = a_{10} e_y e^{-j\beta z} \tag{2-32}$$

$$E_y^- = a_{10} e_y e^{j\beta z} \tag{2-33}$$

$$H_x^+ = -\frac{\lambda}{\lambda_g \eta} E_y^+ \tag{2-34}$$

$$H_x^- = \frac{\lambda}{\lambda_g \eta} E_y^- \tag{2-35}$$

$$e_y = -\frac{\lambda_g \eta}{\lambda} \left(\frac{\lambda\beta}{ab\pi\eta}\right)^{1/2} \sin\frac{\pi x}{a} \tag{2-36}$$

$$h_z = -j\frac{\lambda_g}{2a}\left(\frac{\lambda\beta}{ab\pi\eta}\right)^{1/2} \cos\frac{\pi x}{a} \tag{2-37}$$

$$a_{10} = \frac{j\omega\mu_o}{2} h_z m_z \tag{2-38}$$

Hence, at $x = a/2$ and $z = 0$,

$$E_y^+ = E_y^- = -\frac{k\eta m_z}{ab} \cdot \frac{\lambda_g}{2a} \cdot \cos\frac{\pi x_m}{a} \tag{2-39}$$

$$H_x^+ = -H_x^- = \frac{\lambda}{\lambda_g \eta} E_y^+ \tag{2-40}$$

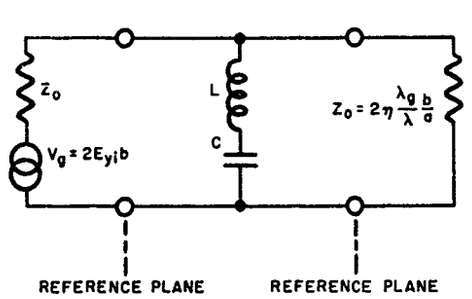

Figure 2-6. Equivalent Circuit for $m = m_z$

The equivalent circuit for the case of $m = m_z$ is shown in Figure 2-6. The Q of the resonant circuit loaded by both terminations is

$$Q_{ex} = \frac{\omega L}{\frac{1}{2}Z_o} = \frac{2\omega L}{Z_o} \qquad (2\text{-}41)$$

The stored energy at resonance is

$$W_m = \frac{1}{2}L\,|I|^2 = \frac{1}{2}L\left|\frac{V_g}{Z_o}\right|^2 = \frac{2L\left|E_{yi}\right|^2 b^2}{Z_o^2} \qquad (2\text{-}42)$$

With Eqs. 2-4, 2-19, 2-26, 2-39, and 2-42 substituted in Eq. 2-41, we obtain for the z-directed dipole:

$$Q_{ex} = \frac{\omega W_m Z_o}{b^2\left|E_{yi}\right|^2} = \frac{ab\lambda_g}{2\pi F_z \cos^2\left(\frac{\pi x_m}{a}\right)} \cdot \left(\frac{2a}{\lambda_g}\right)^2 \qquad (2\text{-}43)$$

Note that in this case Q_{ex} is minimum when the resonant dipole is near a side wall, and is infinite (denoting zero coupling to the incident wave) when the dipole is at the center of the cross section.

2.3 Band-Stop Filter Design

In a practical band-stop filter it is most convenient for the n dielectric resonators to be identical. The variations in Q_{ex} required by Eq. 2-1 can be achieved by proper location of each resonator in the waveguide cross section. For an x-directed dipole moment

$Q_{ex} \propto 1/\sin^2\left(\frac{\pi x_m}{a}\right)$, while for a y-directed dipole moment $Q_{ex} \propto 1/\cos^2\left(\frac{\pi x_m}{a}\right)$.

Variation of Q_{ex} can also be achieved by tilting the dipole axis with respect to the incident magnetic field component. This is especially simple when the dipole is on the waveguide center line, where H_x is maximum and H_z is zero. The x component of m is $m_x = m \cos\theta$ where θ is the angle of the vector m with respect to the x axis. Therefore $F_x = F \cos^2\theta$, and by Eq. 2-28, Q_{ex} of the dipole at $x_m = a/2$ is

$$Q_{ex} = \frac{ab\lambda_g}{2\pi F \cos^2\theta} \qquad (2\text{-}44)$$

Figure 2-7 shows four ways that dielectric-disk resonators can be used in a waveguide band-stop filter. In the usual filter design, Eq. 2-1 requires the center resonator to have the lowest Q_{ex} value, with Q_{ex} of the other resonators in an increasing progression toward each end of the filter. Also, usually $Q_{ex_1} = Q_{ex_n}$, $Q_{ex_2} = Q_{ex_{n-1}}$, etc. The configurations in Figure 2-7 meet these conditions. Various modifications and combinations of Figure 2-7 are possible. For example, instead of $x_1 = x_3$ or $\theta_1 = \theta_3$, one may have $x_1 = a - x_3$ and $\theta_1 = -\theta_3$.

Of the configurations in Figure 2-7, the transversely oriented one shown in (a) appears most convenient. The disks can be supported by polyfoam, or by x-directed metallic or dielectric pins attached to one or both side walls.

2.4 Experimental Band-Stop Filter

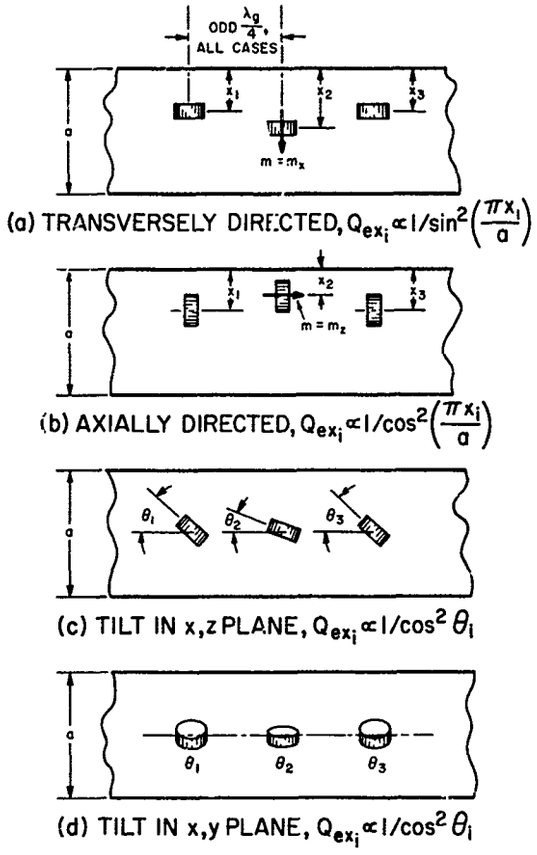

Figure 2-7. Band-Stop Filter Configurations in Waveguide

A three-element band-stop filter was assembled in the transverse configuration of Figure 2-7a. The same prototype low-pass filter and the same dielectric disks were used as in the TEM-mode band-stop filter described in the Fifth and Sixth Quarterly Reports.[4,2] Thus, n = 3 and the pass-band ripple is 0.01 db. The relations between the Q_{ex} values and the bandwidths are as follows:[4]

$$Q_{ex_1} = Q_{ex_3} = 1.544\, Q_{ex_2} \qquad (2\text{-}45)$$

$$w_{0.01db} = \frac{2.06}{Q_{ex_2}} \qquad (2\text{-}46)$$

$$w_{3db} = \frac{1.093}{Q_{ex_2}} \qquad (2\text{-}47)$$

The dielectric disks have parameters $\epsilon_r = 85.6$, D = 0.393 in., and L = 0.235 in. (avg). When placed near the center of a WR-284 waveguide, they resonate near 3210 Mc ($\lambda_o = 3.68$ in.). By Eq. 2-27, the parameter F is therefore approximately

$$F = \frac{0.927 \times 0.393^4 \times 0.235 \times 85.6}{3.68^2} = 0.0329 \text{ in}^3$$

In the experimental filter, the middle disk was placed at the center of the cross section ($x_2 = a/2 = 2.840/2 = 1.420$ in.). The theoretical value of Q_{ex_2} is given by Eq. 2-28 as follows

$$Q_{ex_2} = \frac{ab\lambda_g}{2\pi F \sin^2\left(\frac{\pi}{2}\right)} = \frac{2.84 \times 1.340 \times 4.81}{2\pi \times 0.0329} = 88.6$$

The position of the end disks is determined from Eq. 2-28 to give the desired ratio of Q_{ex_1} to Q_{ex_2}. Thus

$$Q_{ex_1} = 1.544\, Q_{ex_2} = 137.0$$

$$\frac{\sin^2\left(\frac{\pi}{2}\right)}{\sin^2\left(\frac{\pi x_1}{a}\right)} = 1.544$$

$$\sin \frac{\pi x_1}{a} = \frac{1}{\sqrt{1.544}}$$

$$x_1 = 0.297a = 0.845 \text{ in}$$

By means of Eq. 2-47, the 3-db bandwidth is predicted to be

$$BW_{3db} = \frac{1.093}{Q_{ex_2}} \times 3210 = 39.6 \text{ Mc}$$

A polyfoam slab was machined to support the disks in their proper positions. The width and height of the slab are equal to a and b/2, respectively. Longitudinal grooves were cut to hold the disks. The groove depth is D/2, the width is L, and the spacings of the center of each groove from one side of the slab are $x_1 = x_3 = 0.845$ in. and $x_2 = a/2 = 1.420$ in.

First, the resonators were tested individually in their respective locations. The resonant frequencies were found to be not quite equal, differing by 10 Mc from the highest to lowest value. Before proceeding further, the resonant frequencies were equalized by applying small pieces of aluminum foil tape to the surface of two of the disks, thus raising their resonant frequencies to the same value as the third. The tape was attached to one face of each disk at a point about D/4 from the center of the face. Pieces about 0.040×0.040 inch proved sufficient. The particular tape used was "Scotch Sensing Tape", which has a thickness of about 0.0008 in., including its very thin coating of pressure-sensitive adhesive. Judging by the relatively small area of the foil segment and the very small f_o change it causes, the effect on F and Q_u should be negligible. The final f_o and Q_{ex} data are tabulated below.

Disk	f_o	(Q_{ex}) Meas	(Q_{ex}) Theor	$\frac{(Q_{ex})\ \text{Theor}}{(Q_{ex})\ \text{Meas}}$
1	3216.5 Mc	140.7	137.0	0.975
2	3215.4	96.5	88.6	0.920
3	3216.3	147.3	137.0	0.930

The maximum disagreement of the theoretical from the measured values of Q_{ex} is only 8 percent. This is satisfactory confirmation of Eq. 2-28, considering the approximations used in the analysis.

Next, the three disks were inserted in the polyfoam slab with longitudinal axis spacings of $3\lambda_{go}/4 = 3.61$ in. The insertion loss and VSWR responses were measured without any further tuning or other adjustment, and are shown plotted versus frequency in Figures 2-8 and 2-9. The VSWR response is asymmetrical, being well matched in the lower pass band, and having a peak of 1.58 in the upper pass band. Ideally, the filter should have VSWR ripples of 1.10 maximum in both pass bands. It is quite certain that the equal-ripple response could be approximated if small adjustments were made in f_{oi} and x_i. In fact,

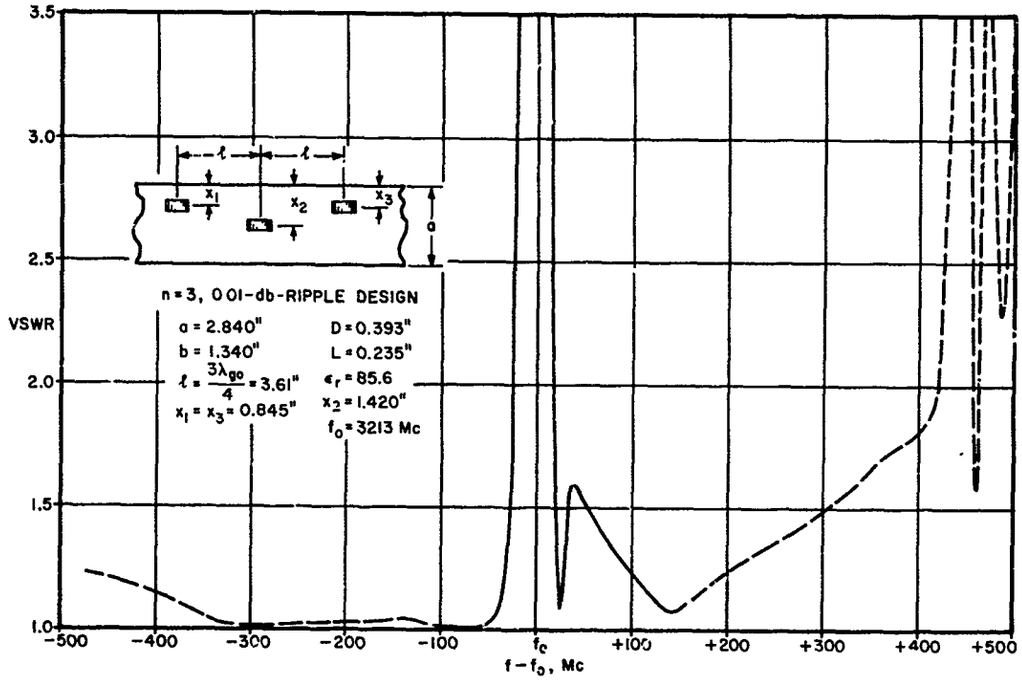

Figure 2-8. VSWR Response of Experimental Band-Stop Filter

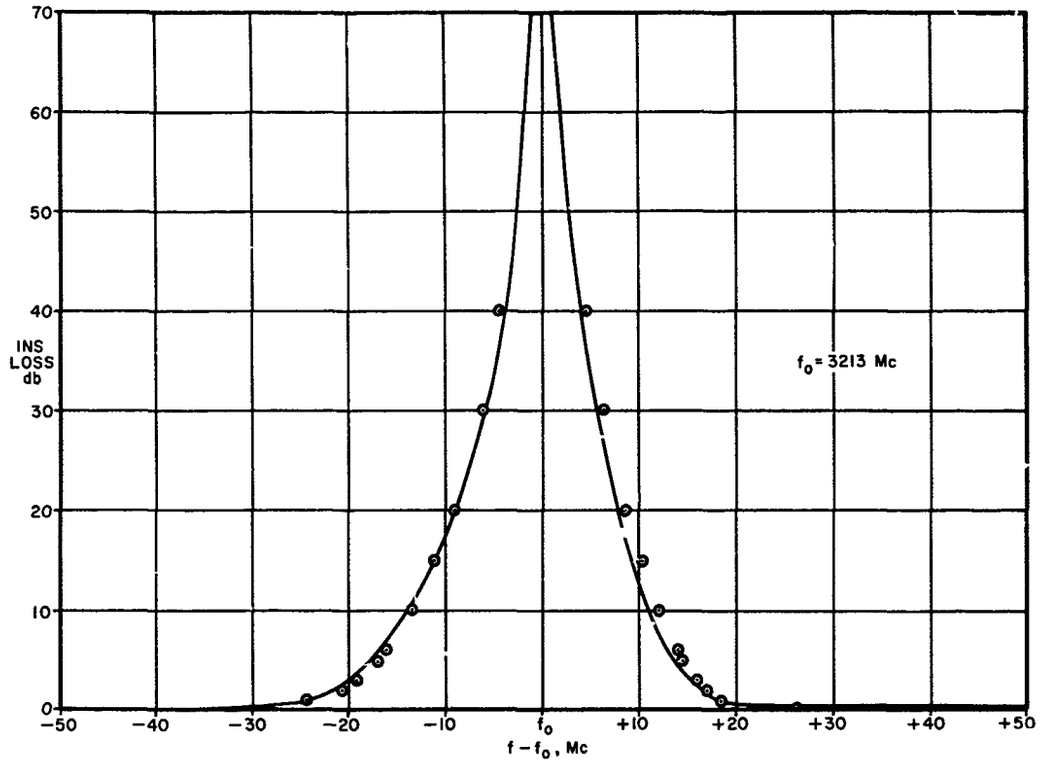

Figure 2-9. Insertion Loss Response
of Experimental Band-Stop Filter

the swept response observed prior to tuning the individual resonators by means of foil tape indicated a well matched upper pass band and a peak in the lower pass band; this is opposite to the case plotted in Figure 2-8.

The VSWR peaks at about 3650 Mc are due to the next mode of resonance in the disks. In this mode, the magnetic-dipole vector is perpendicular to the disk axis. Note that a pair of identical but orthogonal field distributions can exist in this mode, with their

respective m vectors at right angles to each other as well as at right angles to the disk axis. If perfect cylindrical symmetry is maintained, these two resonant-field configurations can exist simultaneously with no coupling or interaction between them. This dual mode may be referred to as a degenerate pair of resonances, to use the terminology of the analogous waveguide-cavity situation. Further discussion of this dual mode is given in Sub-sections 3 and 4 of this report.

The measured insertion-loss bandwidth (Figure 2-9) is 35.1 Mc at the 3-db points. This is 11 percent less than the predicted bandwidth of 39.6 Mc. The following tabulation gives the theoretical ratios of BW_{3db}/BW at various insertion-loss levels for the prototype three-element, 0.01 db-ripple response function. The next two columns give the bandwidths based on these ratios and the theoretical 3-db bandwidth of 39.6 Mc in one case and the measured bandwidth of 35.1 Mc in the other case. The last column gives the actual measured bandwidths.

Ins Loss	Theoretical BW_{3db}/BW	Bandwidths Calculated from BW_{3db}		Measured Bandwidth
		BW_{3db} = 39.6 Mc	BW_{3db} = 35.1 Mc	
3 db	1.00	39.6 Mc	35.1 Mc	35.1 Mc
10	1.38	28.7	25.5	25.5
20	2.02	19.60	17.35	17.7
30	2.94	13.47	11.93	12.3
40	4.26	9.30	8.23	9.0
70	13.60	2.92	2.59	2.0

Comparison of the columns shows good agreement at all insertion-loss levels between the measured data and the data computed from the prototype response function and BW_{3db} = 35.1 Mc. The theoretical bandwidths

based on BW_{3db} = 39.6 Mc are about 11 percent wider on the average. This degree of design accuracy is sufficient for most practical purposes, and is comparable with that achieved in the design of many other kinds of microwave filters.

3. Directional Filters Using Dielectric Resonators

a. Basic Properties of Directional Filters

A directional filter is a reciprocal four-port device combining the properties of a directional coupler, a band-pass filter, and a band-stop filter. A number of waveguide, strip-line, and lumped-constant forms of directional filters have been described in the literature.[6,9] In all cases, the properties depend upon the use of resonant circuits or resonant modes used in pairs, coupled effectively in series and shunt with two equivalent transmission lines.

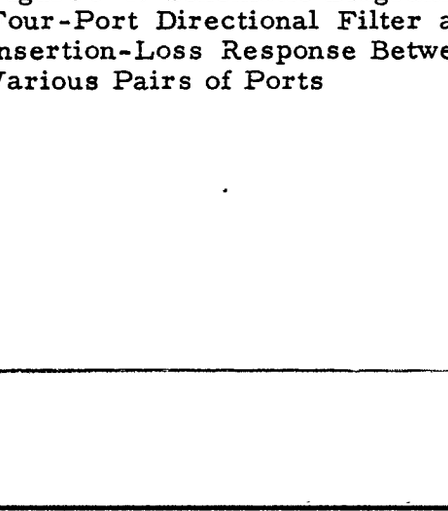

Figure 3-1. Schematic Diagram of Four-Port Directional Filter and Insertion-Loss Response Between Various Pairs of Ports

Figure 3-1 shows a schematic representation of a directional filter, and the response at the various ports. Between Ports 1 and 2 or 3 and 4 a band-stop response is obtained, while between 1 and 3 or 2 and 4 the response is band pass. Ideally, Port 4 is isolated from Port 1 and Port 3 is isolated from Port 2. Each port is reflectionless when the other three ports are terminated in their Z_o loads.

b. Dielectric Directional-Filter Configurations

Several ways that dielectric resonators can be used in directional filters are shown in Figures 3-2 and 3-3. In Figure 3-2, pairs of disks are placed in openings between two waveguides so as to achieve the desired combination of H_x and H_z (series and shunt) couplings. The disks resonate in their fundamental mode, with magnetic-dipole moments along the disk axes. For proper directional-filter performance the resonant frequencies of the two disks should be identical, and the disks should be located in the waveguide structure so that their Q_{ex} values are the same.

The configurations in Figure 3-3 utilize single dielectric elements operating at their second resonance, where a dual, degenerate pair of orthogonal modes can exist independently and simultaneously. The respective pair of magnetic dipoles are perpendicular to each other and to the axis of the disk. These degenerate modes were discussed earlier in this report in connection with the response curve in Figure 2-8.

An analysis of the two-disk configuration of Figure 3-2a is given below. The solution is then extended to some of the other configurations of Figures 3-2 and 3-3. The remaining cases may be treated in a similar manner.

c. Analysis of Two-Disk Directional Filter

Figure 3-4 shows the arrangement of Figure 3-2a with incident-wave voltage amplitudes a_1, a_2, a_3, a_4 and reflected-wave voltage amplitudes b_1, b_2, b_3, b_4 at the ports. (These symbols are according to the usual scattering matrix notation and should not be confused with the waveguide dimensions a and b.) Consider an input

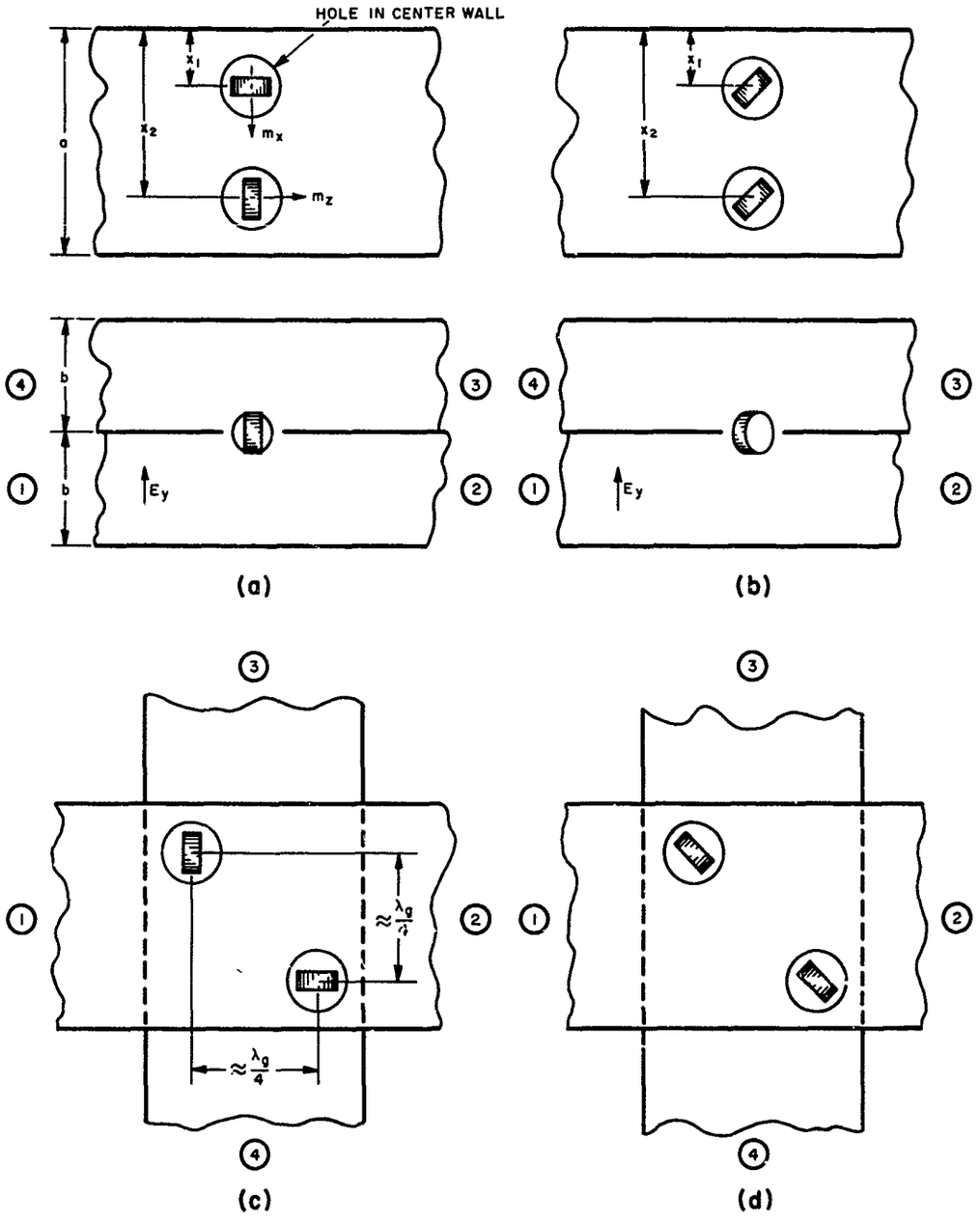

Figure 3-2. Arrangements of Pairs of Dielectric Disks Yielding Directional-Filter Response in Waveguide

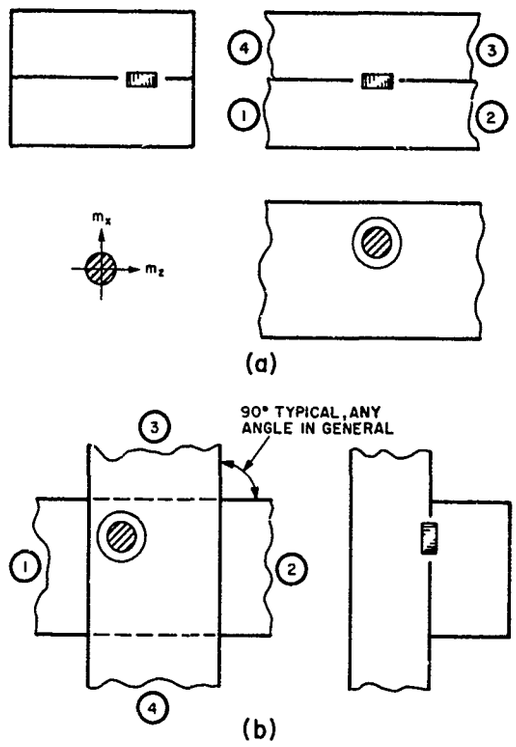

Figure 3-3. Single-Disk, Dual-Mode Configurations Yielding Directional-Filter Response in Waveguide

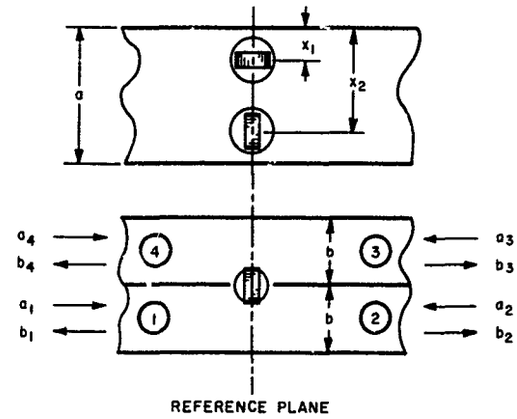

Figure 3-4. Two-Disk Case with In- and Out-Going Wave Amplitudes Defined

wave at Port 1, only. Then $a_1 \neq 0$, while $a_2 = a_3 = a_4 = 0$. The simplest analytical approach to this problem is to obtain solutions for various basic symmetrical and anti-symmetrical excitations and to superimpose these cases to achieve the desired Port 1 excitation. Three basic excitations are sufficient.

The first excitation, shown in Figure 3-5, has $a_1' = a_2' = a_3' = a_4' = 1$. At the reference plane, the total H field has components $H_x = 0$ and $H_z = \max$. Therefore, only m_z is excited, and m_x can be disregarded. The field distribution for this excitation is such that the thin common wall can be eliminated with no effect. Thus, the dielectric resonator denoted by m_z is effectively at the center of a rectangular waveguide of height $b' = 2b$ and width $a' = a$. The equivalent circuit is given in Figure 3-5c. Because of the symmetrical

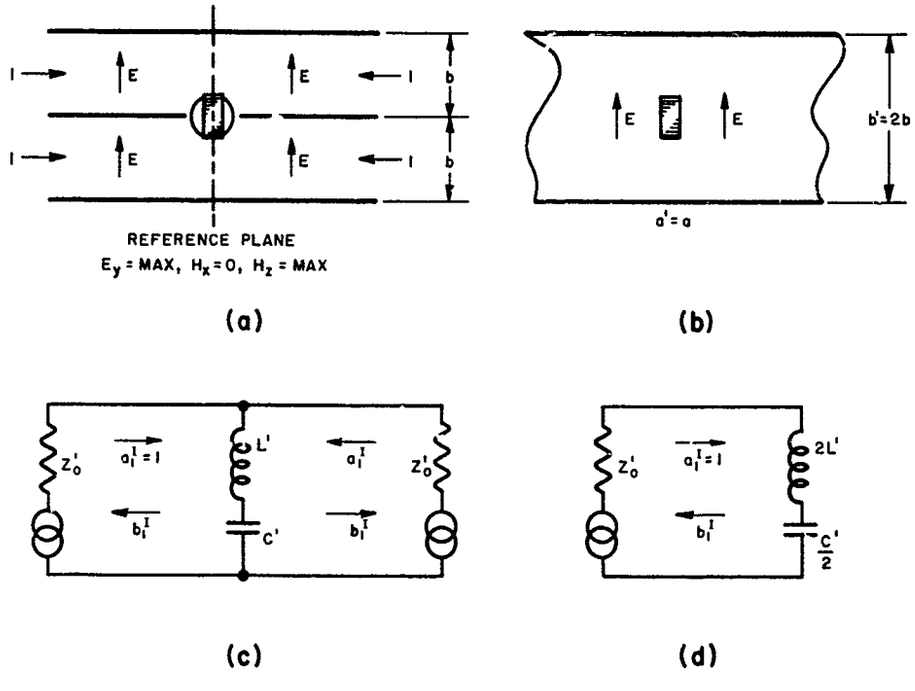

Figure 3-5. First Basic Excitation

excitation, this circuit may be bisected as in Figure 3-5d. It is now apparent that the wave amplitude b_1^I is equal to the reflection coefficient computed from the final circuit. Thus, for this first basic excitation

$$b_1^I = \rho^I = \frac{j2\left(\omega L' - \frac{1}{\omega C'}\right) Z_o'}{j2\left(\omega L' - \frac{1}{\omega C'}\right) + Z_o'}$$

$$= - \frac{1 - j\frac{2\omega L'}{Z_o'}\left(1 - \frac{\omega_o^2}{\omega^2}\right)}{1 + j\frac{2\omega L'}{Z_o'}\left(1 - \frac{\omega_o^2}{\omega^2}\right)} \qquad (3\text{-}1)$$

and

$$\left|b_1^{\prime}\right| = 1 \tag{3-2}$$

$$\angle b_1^{\prime} = 180^{\circ} - 2\tan^{-1}\left(Q_{ex}^{\prime} w\right) \tag{3-3}$$

where $Q_{ex}^{\prime}$ is the external Q of the magnetic dipole in the waveguide of height b' and width a' (as in Eq. 2-41), and $w = \left(f_2 - f_1\right)/f_o$ is the relative bandwidth between corresponding frequencies f_1 and f_2. (In the narrow-band case, $f_2 - f_o = f_o - f_1$.)

The second basic excitation, shown in Figure 3-6, has $a_1^{II} = a_4^{II} = 1$ and $a_2^{II} = a_3^{II} = -1$. In this anti-symmetrical case, total H at the reference plane has components H_x = max and $H_z = 0$, and hence m_x is excited and m_z can be disregarded. Again the thin common wall may be removed with no effect, leaving m_x at the center of a rectangular waveguide of height b' = 2b and width a' = a. The equivalent circuit is given in Figure 3-6c, and its bisected form is given in Figure 3-6d. In this case,

$$b_1^{II} = \rho^{II} = \frac{Y_o^{\prime} - j2\left(\omega C^{\prime} - \frac{1}{\omega L^{\prime}}\right)}{Y_o^{\prime} + j2\left(\omega C^{\prime} - \frac{1}{\omega L^{\prime}}\right)}$$

$$= \frac{1 - j\frac{2\omega C^{\prime}}{Y_o^{\prime}}\left(1 - \frac{\omega_o^2}{\omega^2}\right)}{1 + j\frac{2\omega C^{\prime}}{Y_o^{\prime}}\left(1 - \frac{\omega_o^2}{\omega^2}\right)} \tag{3-4}$$

and

$$\left|b_1^{II}\right| = 1 \tag{3-5}$$

$$\angle b_1^{II} = -2\tan^{-1}\left(Q'_{ex}w\right) \tag{3-6}$$

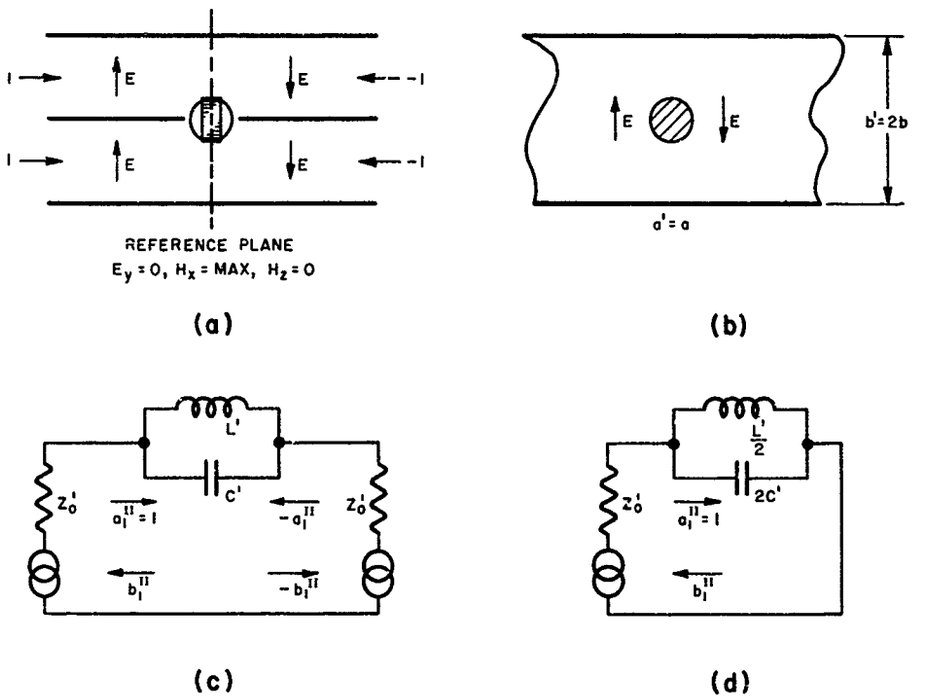

Figure 3-6. Second Basic Excitation

The third excitation, shown in Figure 3-7, has $a_1 = 1$, $a_4 = -1$, $a_2 = 0$, and $a_3 = 0$. With this excitation, all field components are zero at the centers of the holes in the common wall. Hence, neither m_x nor m_y is excited, and the equivalent circuit is simply a generator and load with an incident wave and no reflected wave. (The hole and disk are assumed small enough not to give rise to an appreciable second-order reflection.)

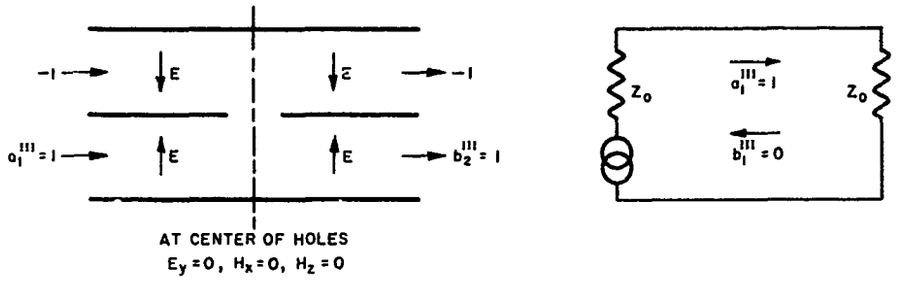

Figure 3-7. Third Basic Excitation

The proper superposition of the three excitations is in the ratio of one unit each of a_1^I and a_1^{II} plus two units of a_1^{III}. The total wave amplitudes are then

$$a_1 = 1 + 1 + 2 = 4$$

$$a_2 = 0$$

$$a_3 = 0$$

$$a_4 = 0$$

$$b_1 = b_1^I + b_1^{II}$$

$$b_2 = b_1^I - b_1^{II} + 2$$

$$b_3 = b_1^I - b_1^{II} - 2$$

$$b_4 = b_1^I + b_1^{II}$$

Perfect directional-filter performance can be achieved if, and only if, the external Q values and resonant frequencies of the two magnetic dipoles are equal. Then Eqs. 3-3 and 3-6 become

$$\angle b_1^{II} = -2\tan^{-1}\left(Q'_{ex}w\right) = \angle b_1^{I} - 180^{o}, \tag{3-7}$$

and

$$b_1^{I} + b_1^{II} = 0 \tag{3-8}$$

$$b_1^{I} - b_1^{II} = 2b_1^{I} \tag{3-9}$$

Therefore

$$b_1 = 0$$

$$b_2 = 2\left(b_1^{I} + 1\right)$$

$$b_3 = 2\left(b_1^{I} - 1\right)$$

$$b_4 = 0$$

The transmission coefficients between Port 1 and the other three ports are

$$t_{12} = \frac{1}{2}\left(b_1^{I} + 1\right) \tag{3-10}$$

$$t_{13} = \frac{1}{2}\left(b_1^{I} - 1\right) \tag{3-11}$$

$$t_{14} = 0 \tag{3-12}$$

At f_o, $b_1' = -1$, so that $t_{12} = 0$ and $t_{13} = -1$. The 3-db insertion-loss points occur for both t_{12} and t_{13} at the frequencies where $b_1' = \pm j$ and $b_1' = 90^\circ$ and 270°. With reference to Eq. 3-3, the relative 3-db bandwidth is related to Q'_{ex} by

$$\frac{(f_2 - f_1)_{3db}}{f_o} = w_{3db} = \frac{1}{Q'_{ex}} \tag{3-13}$$

In Sub-section 2 of this report, Q_{ex} of a magnetic-dipole resonator in a rectangular waveguide loaded by Z_o at both ends was evaluated for both m_x and m_y orientations. By Eqs. 2-28 and 2-43, the formulas for Q'_{ex} in waveguides of cross section a' and b' are

$$Q'_{ex_x} = \frac{a'b'\lambda_g}{2\pi F_x \sin^2\left(\frac{\pi x_1}{a}\right)} \qquad (m_x \text{ case}) \tag{3-14}$$

$$Q'_{ex_z} = \frac{a'b'\lambda_g}{2\pi F_z \cos^2\left(\frac{\pi x_2}{a}\right)} \cdot \left(\frac{2a}{\lambda_g}\right)^2 \qquad (m_z \text{ case}) \tag{3-15}$$

Now let $Q'_{ex_x} = Q'_{ex_z} = Q'_{ex}$ and $F_x = F_z = F$, and let $a' = a$ and $b' = 2b$. Then

$$Q'_{ex} = \frac{ab\lambda_g}{\pi F \sin^2\left(\frac{\pi x_1}{a}\right)} = \frac{1}{w_{3db}} \tag{3-16}$$

and

$$\sin \frac{\pi x_1}{a} = \pm \frac{\lambda_g}{2a} \cos \frac{\pi x_2}{a} \tag{3-17}$$

These are the design equations for a two-disk directional filter of the type shown in Figure 3-2a. The factor F is a function of the parameters of the dielectric disk, and may be computed from Eq. 2-27. Note that Q'_{ex} and w_{3db} are respectively twice and half the corresponding values for the same disk functioning as a rejection resonator at the same position in a single waveguide of cross section a and b.

d. Analysis of Single-Disk Dual-Mode Directional Filter

The preceding analysis can easily be extended to cover the single-disk configuration of Figure 3-3a operating in the second resonance, with dual orthogonal modes having magnetic dipole moments $m_x = m_z = m$. The two-disk case is reduced to the single-disk dual-mode case by letting $x_1 = x_2$, so that the two disks coincide. Equations 3-16 and 3-17 then apply, with Eq. 3-17 reducing to

$$\tan \frac{\pi x_1}{a} = \pm \frac{\lambda_g}{2a} \tag{3-18}$$

This relation specifies the proper location of the center of the disk. Two values of x_1 satisfy Eq. 3-18; namely, $(x_1)_1$ and $(x_1)_2 = a - (x_1)_1$. Examination of the H_x and H_z field components (Eqs. 2-11 and 2-37) indicates that at these values of x_1,

$$H_z = -jH_x \text{ and } H_z = jH_x \tag{3-19}$$

This is the condition for circular polarization of the H field. Hence the dual-mode disk placed at one of these points has dipole moments

$$m_z = -jm_x \text{ or } m_z = jm_x \tag{3-20}$$

and thus the dipole moment of the disk is also circularly polarized in the x, z plane.

Equation 3-16 for Q'_{ex} can be simplified with the aid of Eq. 3-18, modified as follows

$$\csc^2\left(\frac{\pi x_1}{a}\right) = 1 + \cot^2\left(\frac{\pi x_1}{a}\right) = 1 + \left(\frac{2}{\lambda_g}\right)^2 = 1 + \left(\frac{\lambda_c}{\lambda_g}\right)^2$$

$$= \left(\frac{2a}{\lambda}\right)^2 \tag{3-21}$$

where use was made of the general relation

$$\frac{1}{\lambda_g^2} = \frac{1}{\lambda^2} - \frac{1}{\lambda_c^2} \tag{3-22}$$

Upon substituting this in Eq. 3-16, we obtain the final formula for Q'_{ex} and w_{3db} of a single-disk dual-mode directional filter, with the disk located according to Eq. 3-18.

$$Q'_{ex} = \frac{1}{w_{3db}} = \frac{4a^3 b \lambda_g}{\pi \lambda^2 F} \tag{3-23}$$

A formula for F in the dual-mode case is not yet available. Experimental data for F will be used until a suitable formula is derived.

Because the m vector of the dual-mode disk is circularly polarized, it is obvious that the two waveguides in Figure 3-3a need not be co-directed. Their axes may be at any angle, as shown in Figure 3-3b, without affecting the directional-filter properties.

Also, a shape other than a disk may be used, as long as it has symmetry about two axes. For example, a square prism (or tile) would be suitable.

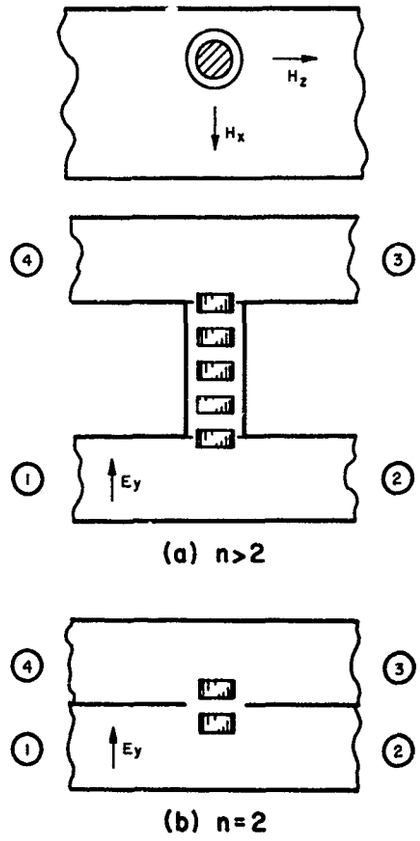

Figure 3-8. Examples of Multi-Resonator Direction Filters Using Dual-Mode Disks

e. Multi-Element Directional Filters

The directional filters shown in Figures 3-2 and 3-3 have response functions characteristic of two-port single-resonator band-pass and band-stop filters. As in the case of other types of directional filters, additional resonators may be coupled in cascade oetween the two waveguides in order to achieve the more complex response functions of multi-resonator, two-port filters. An example of such a design is shown in Figure 3-8a. Five dual-mode (circularly polarized) disks are coupled in cascade within a circular tube below cutoff. The end disks couple to the rectangular waveguides at points of circular polarization of the H field.

If the end disks project half way into the rectangular waveguides, the external Q, Q_{ex_1}, of each end disk loaded by one waveguide is approximately twice the external Q of one disk loaded by two waveguides. The latter external Q is Q'_{ex}, which is given by Eq. 3-23. Hence

$$Q_{ex_1} \approx \frac{8a^3 b\lambda_g}{\pi\lambda^2 F} \tag{3-24}$$

for one dual-mode disk oriented according to Eq. 3-18 and projecting half way into one rectangular waveguide.

For a particular desired response function and bandwidth, the required values of Q_{ex_1} and coupling coefficients $k_{i,i+1}$ may be computed from the elements of the corresponding low-pass prototype filter.[5,6] In the directional filter, Q_{ex_1} can be adjusted by the amount of penetration of the end disks into the rectangular waveguides. The range of adjustment is from somewhat less than the value given by Eq. 3-24 for a disk projecting most of its length into the rectangular waveguide, to infinity for a disk within the cut-off tube separated by a large distance from the rectangular waveguide. The desired values of $k_{i,i+1}$ can be achieved by proper spacing of the disks along the circular tube.

A convenient structure offering the response function of a two-element prototype filter is shown in Figure 3-8b. This utilizes the geometry of Figure 3-8a, but with the length of the cut-off tube reduced to zero. The spacing between the dual-mode disks would be adjusted to achieve the desired maximally flat or ripple response.

f. Practical Design Problems

Prior experience with earlier types of directional filters has shown this kind of device to require very precise adjustment in order to operate well. The resonant modes have to be tuned to the same frequency within a few percent of the 3-db bandwidth. The loaded Q's have to be almost perfectly equal and, furthermore, the loading of

each resonator by each waveguide must be virtually identical. Any direct coupling between the dual resonant modes must be very small.

An experimental directional filter of the single-disk cross-guide type is now being constructed. This will be tested, and the results will be described in the next report.

4. Resonant Modes of Dielectric Cylinders

All of the work described in earlier reports was done with dielectric cylinders in the axial-magnetic-dipole mode of resonance. For L less than D, this is the lowest-frequency (or fundamental) mode of resonance. The second mode of resonance has its magnetic dipole perpendicular to the axis of the cylinder. This mode occurs in degenerate, orthogonal pairs, as discussed in Sub-sections 2 and 3 of this report.

Knowledge of the second mode's behavior is important for two reasons. First, this mode generally causes a spurious response in filters designed to operate with the first mode. Second, this mode is itself useful in certain types of devices, such as the circularly polarized directional filters described in Sub-section 3.

In order to obtain information on the resonant frequencies of the first two modes, a dielectric sample was made having $\epsilon_r = 95$, D = 0.325 in., and an initial length L = 0.500 in. The length was progressively reduced in small amounts, and frequencies f_1, f_2, and f_3 were measured at each value of L. Frequency f_1 applies to the mode having m axially oriented with respect to the cylinder, f_2 applies to the mode having m transverse to the axis, and f_3 applies to the next higher observed resonance. The resulting curves of f_1, f_2, and f_3 versus L are plotted in Figure 4-1.

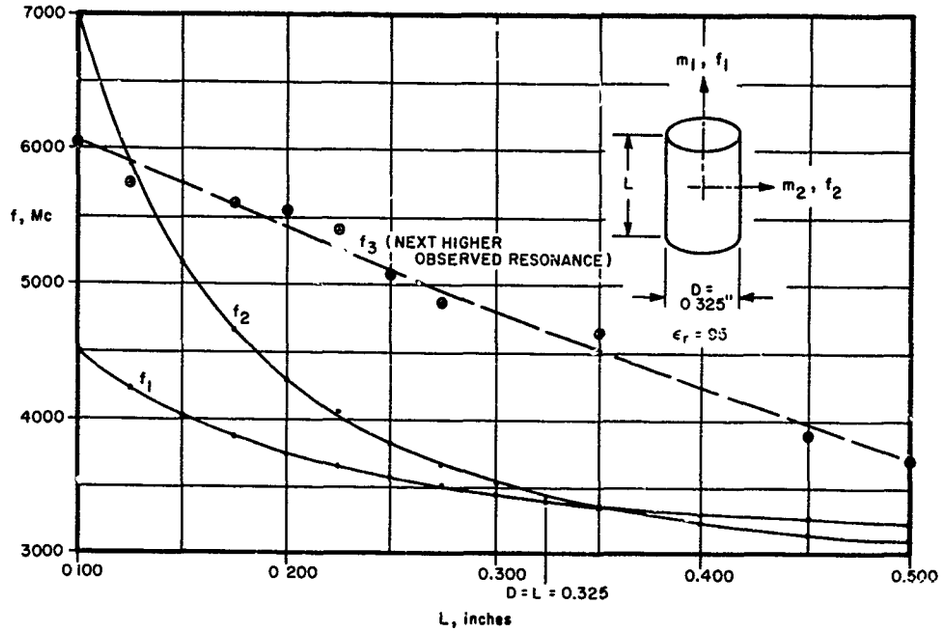

Figure 4-1. First Three Resonant Frequencies Versus Length of a Dielectric Cylinder of Constant Diameter

The curves for f_1 and f_2 behave as expected. For "disk" shapes (i.e., $L < D$), f_2 is greater than f_1, while for "rod" shapes (i.e., $L > D$), f_2 becomes less than f_1. The curves cross at $L = 1.08D$. This behavior is reasonable according to the first-order mode theory of dielectric cylinders discussed in the First Quarterly Report.[3] According to first-order theory, the curves should cross exactly at $L = D$.

The data for the next higher resonant frequency, f_3, does not fall on a smooth curve. The reason for this is not known, but the irregular effect may be due to the presence of several modes close to each other in frequency, or may be due to experimental difficulties in accurately measuring the third resonance.

Study of Figure 4-1 shows that L/D should be less than 0.6 when f_1 is used in a filter design, in order to obtain good separation

from f_2 and f_3. When f_2 is to be used, a length between about 0.160 inch and 0.190 inch gives best separation from f_1 and f_3. The corresponding range of L/D is 0.49 to 0.58. The optimum value of L/D for operation in the second resonance is about 0.54. Another region of separation of f_2 lies beyond L = 0.500 in., where measurements were not made. However, this region does not appear promising, since f_1 and f_2 are diverging very slowly at L = 0.500 in., while f_2 and f_3 are converging.

5. Effect of Metal-Wall Proximity – Axial Case

In the Third Quarterly Report, measured values of Q_u and f_o were presented for a dielectric disk placed in cut-off square waveguides of varying size. The disk axis was transverse to the axis of the waveguide. An approximate analysis of that case was carried out in the Sixth Quarterly Report, with fairly good verification of the experimental data.

Measurements are now complete on a disk placed axially in square and circular cut-off waveguides. The resulting Q_u and f_o data are plotted in Figures 5-1 and 5-2. The disk is the same one used in the transverse-orientation examples of the Third and Sixth Quarterly Reports, and therefore the new data may be compared directly to the previous data.

The Q_u values in Figure 5-1 for the axial disk within a square waveguide are almost identical to the earlier data for the disk placed transversely. However, the effect of the walls on f_o is much greater in the axial case. Both the Q_u and f_o results are in variance with the theoretical formulas derived in the Sixth Quarterly Report (Eqs. (2-48), (2-52), and (2-53) of that report), the measured Q_u values

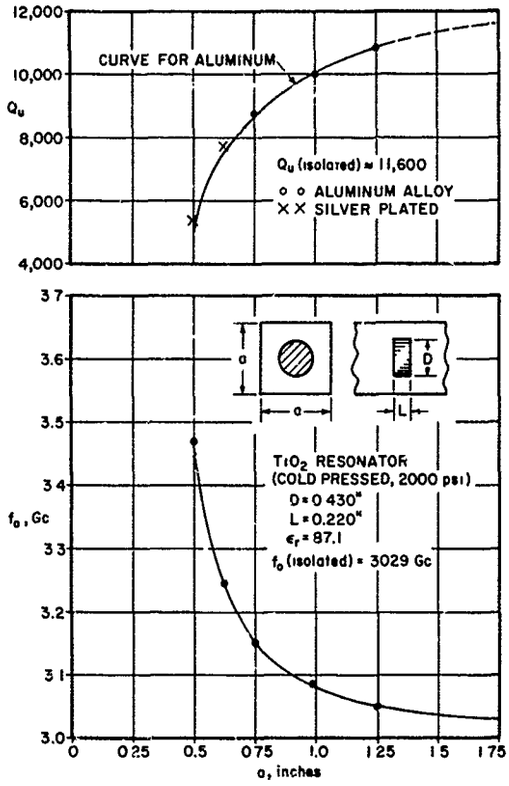

Figure 5-1. Q_u and f_o of a Dielectric Disk Axially Oriented in a Cut-Off Square Tube

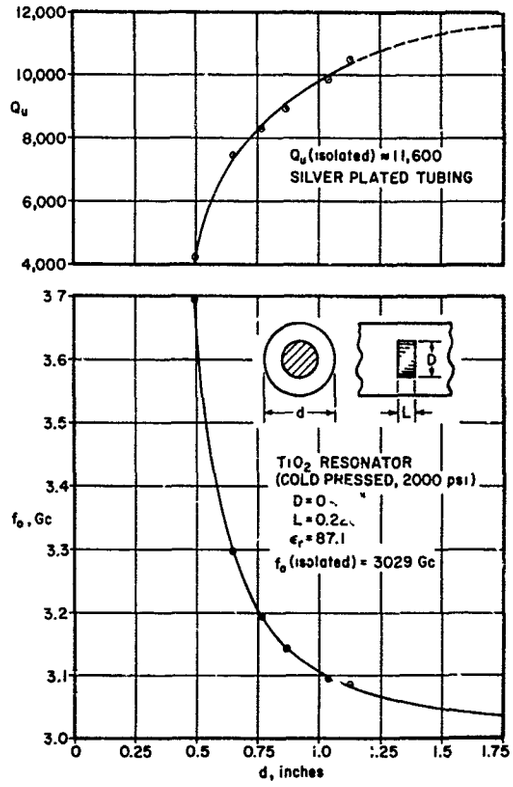

Figure 5-2. Q_u and f_o of a Dielectric Disk Axially Oriented in a Cut-Off Round Tube

being lower and the f_o change being higher. Good agreement, however, had been found for both Q_u and f_o in the transverse case.

The errors in the formulas for the axial case may be attributed to the approximations in the analysis. The principal approximation was the assumption of a single infinite metal wall rather than the actual four-sided square waveguide. Figure 5-3a shows the single image of the equivalent magnetic dipole for the assumed infinite-plane geometry,

and Figure 5-3b shows the infinite array of images for the square-waveguide geometry. All images of the magnetic dipole are in the same direction as the dipole.

In the analysis in the Sixth Quarterly Report, the effect of the single image on wall loss and on resonant-frequency shift was multiplied by four to take account of the effects of the four adjacent images in the actual waveguide boundary. It is apparent from Figure 5-3 that the infinite number of non-adjacent images will also have an effect. This is especially severe for the axial case, since the images are all in the same direction. Thus, the H field on the metal walls of the waveguide will be considerably greater than in the assumed situation, resulting in greater total loss and lower Q_u. Also, the total frequency change will be considerably greater than that caused by only the four adjacent images.

The image situation for the transverse case is shown in Figure 5-4. In this case the images in the infinite array have alternating directions. The result of this alternation is that contributions from the non-adjacent images tend to cancel. Therefore, an analysis based on only the four adjacent images can be expected to have fair accuracy, and the good agreement obtained between theoretical and experimental Q_u and f_o in the transverse case is substantiated.

The analysis of the axial case could be extended to take account of the contributions of the non-adjacent images. This may be undertaken in the future, but the availability of the experimental data makes this task less important than other items currently of interest.

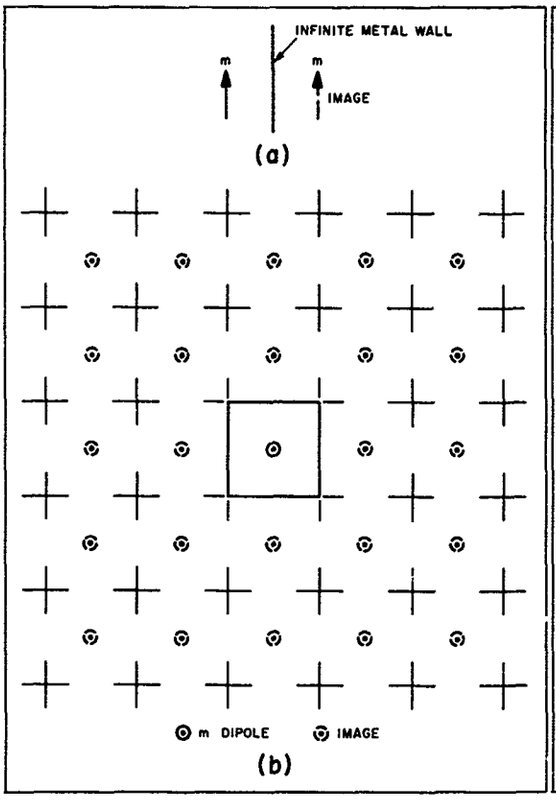

Figure 5-3. Images, Axial Orientation; (a) Magnetic Dipole and its Image in a Single Infinite Wall (b) Dipole and its Infinite Array of Images in the Walls of a Square Waveguide

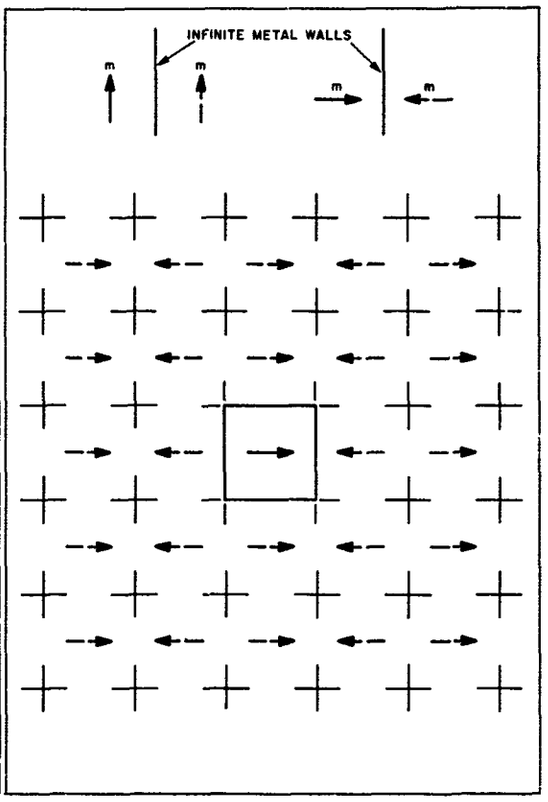

Figure 5-4. Images, Transverse-Orientation in a Square Waveguide

SECTION V

CONCLUSIONS

Dielectric-resonator band-stop filters in waveguide are shown to be feasible, and design formulas derived for them are shown to be sufficiently accurate for practical purposes. Although a dielectric resonator band-stop filter has the same length as a conventional waveguide band-stop filter, it eliminates the need for external cavities. Both types offer approximately the same unloaded Q and dissipation-loss characteristics. The dielectric-resonator assembly can be easily inserted into a length of straight waveguide. Suitable lengths would usually be available in waveguide assemblies, and thus no additional space would be required for the band-stop filter.

Waveguide directional filters utilizing dielectric resonators are shown to be feasible. A number of possible configurations are given. Some use resonators in pairs, while others use single dielectric objects operating in the second "dual" mode of resonance. Additional resonators may be added to achieve multi-resonator response. It is shown that the analysis on band-stop filters can be extended to cover directional filters as well. Design formulas are derived for directional-filter cases of particular interest. Many difficulties exist in the alignment of this type of filter, and a conclusion on practical feasibility will be made in the next report after an experimental study is completed.

Of the infinite number of resonances occurring in a dielectric object, only the first two appear to be of practical value for filters. The first (or lowest frequency) mode in a dielectric disk would be used in most filter designs. The second mode would have more limited applicability in special types of filters, such as directional filters. The particular feature of interest of this second mode is its dual, orthogonal nature; that is, the ability of this mode to occur simultaneously

in two independent field distributions at the same frequency. The resonant-frequency curves show the first mode to be well separated from the second when the L/D ratio of the disk is below 0.6. The range of L/D for good separation of the second from the first and third modes is quite small, being about 0.49 to 0.58, with the optimum ratio at about 0.54. In the latter case, the adjacent-mode frequencies are at about plus and minus 18 percent from the second-mode frequency. In addition to the disk shape, any other shape offering two-axis symmetry can support dual, orthogonal resonances at the same frequency. An example is the square prism or "tile" shape.

The measured Q_u values for an axially oriented disk in square cut-off waveguides of varying size are almost identical to that obtained for the transverse orientation. The effect on resonant frequency, however, is greater in the axial case. Both of these results are in substantial disagreement with the previously developed theory. The fact that the theory gives good results in the transverse case but not the axial case can be explained in terms of the assumption that only the four adjacent images in the infinite array of equivalent magnetic-dipole images need be considered. In the transverse case the directions of the images alternate, with the effect that contributions from non-adjacent images tend to cancel each other. In the axial case all images have the same direction, so that contributions from non-adjacent images should not be disregarded. Because the measured curves are useful in themselves, the task of extending the theory to take account of the non-adjacent images has been assigned a low priority.

SECTION VI

PROGRAM FOR NEXT INTERVAL

Further analysis and experimental study will be made of dielectric-resonator directional-filter configurations in waveguide and strip line. Investigation of band-pass end-loading techniques will continue. An analysis of axially oriented resonators in cut-off circular tubes will be included in the next report. Several experimental band-pass, band-stop, and diplexer filters will be constructed for delivery.

SECTION VII

LIST OF REFERENCES

1. S. B. Cohn and K. C. Kelly, "Investigation of Microwave Dielectric-Resonator Filters," Third Quarterly Report on Contract DA-36-039-AMC-02267(E), 1 January 1964 to 31 March 1964, Rantec Corp., Project 31625.

2. S. B. Cohn and E. N. Torgow, "Investigation of Microwave Dielectric-Resonator Filters," Sixth Quarterly Report on Contract DA-36-039-AMC-02267(E), 1 December 1964 to 28 February 1965, Rantec Corp., Project 31625.

3. S. B. Cohn and C. W. Chandler, "Investigation of Microwave Dielectric-Resonator Filters," First Quarterly Report on Contract DA-36-039-AMC-02267(E), 1 July 1963 to 30 September 1963, Rantec Corp., Project 31625.

4. S. B. Cohn and E. N. Torgow, "Investigation of Microwave Dielectric-Resonator Filters," Fifth Quarterly Report on Contract DA-36-039-AMC-02267(E), 1 September 1964 to 30 November 1964, Rantec Corp., Project 31625.

5. S. B. Cohn, "Direct-Coupled-Resonator Filters," Proc. IRE, Vol. 45, pp. 187 - 196, February 1957.

6. G. Matthaei, L. Young, and E. M. T. Jones, "Microwave Filters, Impedance-Matching Networks and Coupling Structures," McGraw-Hill Book Co., New York, 1964.

7. S. B. Cohn and K. C. Kelly, "Investigation of Microwave Dielectric-Resonator Filters," Second Quarterly Report on Contract DA-36-039-AMC-02267(E), 1 October 1963 to 31 December 1963, Rantec Corp., Project 31625.

8. S. B. Cohn and E. N. Torgow, "Investigation of Microwave Dielectric-Resonator Filters," Fourth Quarterly Report on Contract DA-36-039-AMC-02267(E), 1 April 1964 to 31 August 1964, Rantec Corp., Project 31625.

9. S. B. Cohn and F. S. Coale, "Directional Channel Separation Filters," Proc. IRE, Vol 44, pp. 1018 - 1024, August 1956.

SECTION VIII

IDENTIFICATION OF KEY TECHNICAL PERSONNEL

	Hours
Dr. Seymour B. Cohn Specialist	90
Mr. Eugene N. Torgow Staff Engineer	128
Mr. Richard V. Reed Engineer	22
Mr. Howard V. Stein Junior Engineer	261.5

Unclassified
Security Classification

DOCUMENT CONTROL DATA - R&D
(Security classification of title, body of abstract and indexing annotation must be entered when the overall report is classified)

1 ORIGINATING ACTIVITY *(Corporate author)* Rantec Corporation Calabasas, California	2a REPORT SECURITY CLASSIFICATION Unclassified 2b GROUP

3 REPORT TITLE

Investigation of Microwave Dielectric-Resonator Filters

4 DESCRIPTIVE NOTES *(Type of report and inclusive dates)*

Seventh Quarterly Report 1 March 65 - 31 May 65

5 AUTHOR(S) *(Last name, first name, initial)*

Cohn, Seymour B.
Torgow, Eugene N.

6 REPORT DATE	7a TOTAL NO. OF PAGES	7b NO OF REFS
28 July 1965	50	9

8a CONTRACT OR GRANT NO. DA 36-039 AMC-02267(E) b PROJECT NO IP6 22001 A 057 c IP6 22001 A 057 02 d.	9a ORIGINATOR'S REPORT NUMBER(S) 9b OTHER REPORT NO(S) *(Any other numbers that may be assigned this report)*

10 AVAILABILITY/LIMITATION NOTICES

Qualified requestors may obtain copies of this report from DDC.
DDC release to CFSTI not authorized.

11 SUPPLEMENTARY NOTES	12. SPONSORING MILITARY ACTIVITY
	U. S. Army Electronics Command Fort Monmouth, N. J. (AMSEL-KL-EM)

13 ABSTRACT

Waveguide band-stop filters using dielectric resonators are considered. Two basic orientations, transverse and axial, of a dielectric resonator in a TE_{10}-mode rectangular waveguide are analyzed. Formulas for external Q are derived in both cases. The experimental response of a three resonator band-stop filter is shown to agree well with the theoretically anticipated performance.

Various configurations of dielectric resonators in waveguide that yield directional filter performance are described. Pairs of resonators operating in their fundamental mode are used as well as a single resonator operating in its second mode of resonance. Formulas are derived for several cases.

Measured resonant frequency curves are presented for the first three modes of a disk as a function of length-to-diameter ratio and favorable regions of L/D yielding good mode separation are found for the cases of the first and second modes.

Data showing the effect of metal-wall proximity on unloaded Q and resonant frequency are presented for an axially oriented dielectric disk in square and circular tubes below cut-off.

DD FORM 1 JAN 64 1473

Unclassified
Security Classification

14 KEY WORDS	LINK A		LINK B		LINK C	
	ROLE	WT	ROLE	WT	ROLE	WT
Filter						
Dielectric						
Resonator						
Dielectric Resonator						
Unloaded Q						

INSTRUCTIONS

1. ORIGINATING ACTIVITY: Enter the name and address of the contractor, subcontractor, grantee, Department of Defense activity or other organization *(corporate author)* issuing the report.

2*a*. REPORT SECURITY CLASSIFICATION: Enter the overall security classification of the report. Indicate whether "Restricted Data" is included. Marking is to be in accordance with appropriate security regulations.

2*b*. GROUP: Automatic downgrading is specified in DoD Directive 5200.10 and Armed Forces Industrial Manual. Enter the group number. Also, when applicable, show that optional markings have been used for Group 3 and Group 4 as authorized.

3. REPORT TITLE: Enter the complete report title in all capital letters. Titles in all cases should be unclassified. If a meaningful title cannot be selected without classification, show title classification in all capitals in parenthesis immediately following the title.

4. DESCRIPTIVE NOTES: If appropriate, enter the type of report, e.g., interim, progress, summary, annual, or final. Give the inclusive dates when a specific reporting period is covered.

5. AUTHOR(S): Enter the name(s) of author(s) as shown on or in the report. Enter last name, first name, middle initial. If military, show rank and branch of service. The name of the principal author is an absolute minimum requirement.

6. REPORT DATE: Enter the date of the report as day, month, year; or month, year. If more than one date appears on the report, use date of publication.

7*a*. TOTAL NUMBER OF PAGES: The total page count should follow normal pagination procedures, i.e., enter the number of pages containing information.

7*b*. NUMBER OF REFERENCES: Enter the total number of references cited in the report.

8*a*. CONTRACT OR GRANT NUMBER: If appropriate, enter the applicable number of the contract or grant under which the report was written.

8*b*, 8*c*, & 8*d*. PROJECT NUMBER: Enter the appropriate military department identification, such as project number, subproject number, system numbers, task number, etc.

9*a*. ORIGINATOR'S REPORT NUMBER(S): Enter the official report number by which the document will be identified and controlled by the originating activity. This number must be unique to this report.

9*b*. OTHER REPORT NUMBER(S): If the report has been assigned any other report numbers *(either by the originator or by the sponsor)*, also enter this number(s).

10. AVAILABILITY/LIMITATION NOTICES: Enter any limitations on further dissemination of the report, other than those imposed by security classification, using standard statements such as:

(1) "Qualified requesters may obtain copies of this report from DDC."

(2) "Foreign announcement and dissemination of this report by DDC is not authorized."

(3) "U. S. Government agencies may obtain copies of this report directly from DDC. Other qualified DDC users shall request through _____."

(4) "U. S. military agencies may obtain copies of this report directly from DDC. Other qualified users shall request through _____."

(5) "All distribution of this report is controlled. Qualified DDC users shall request through _____."

If the report has been furnished to the Office of Technical Services, Department of Commerce, for sale to the public, indicate this fact and enter the price, if known.

11. SUPPLEMENTARY NOTES: Use for additional explanatory notes.

12. SPONSORING MILITARY ACTIVITY: Enter the name of the departmental project office or laboratory sponsoring *(paying for)* the research and development. Include address.

13 ABSTRACT: Enter an abstract giving a brief and factual summary of the document indicative of the report, even though it may also appear elsewhere in the body of the technical report. If additional space is required, a continuation sheet shall be attached.

It is highly desirable that the abstract of classified reports be unclassified. Each paragraph of the abstract shall end with an indication of the military security classification of the information in the paragraph, represented as *(TS)*, *(S)*, *(C)*, *or (U)*.

There is no limitation on the length of the abstract. However, the suggested length is from 150 to 225 words.

14. KEY WORDS. Key words are technically meaningful terms or short phrases that characterize a report and may be used as index entries for cataloging the report. Key words must be selected so that no security classification is required. Identifiers, such as equipment model designation, trade name, military project code name, geographic location, may be used as key words but will be followed by an indication of technical context. The assignment of links, rules, and weights is optional.